

## Synthesis of TiO<sub>2</sub>/ZnO Nanocomposites by the Electrochemical Method and Their Application in Dye-Sensitized Solar Cells (DSSCs)

Aqeel Mahdi Jreo Alduhaidahawi<sup>1</sup> and Ali Abdulsalam Ahmed<sup>2\*</sup>

<sup>1</sup>Department of Chemistry, College of Science, Kufa University, Najaf 54001, Iraq

<sup>2</sup>Ministry of Education, Rusafa Second Directorate of Education, Baghdad 10045, Iraq

\* Corresponding author:

email:

alia.alhussaini@student.uokufa.edu.iq

Received: July 19, 2023

Accepted: September 8, 2023

DOI: 10.22146/ijc.87071

**Abstract:** Various standard methods have previously been used for the synthesis of nanoparticles that produce unhealthy waste. They are also considered unsafe and expensive methods. An alternative technology is needed to synthesize nanoparticles that consume less energy and are more environmentally friendly. In this research, a TiO<sub>2</sub>/ZnO nanocomposite has been synthesized, which was produced with efficient energy and no environmental pollution using an easy and fast method (electrochemical). Additionally, dye-sensitized solar cells (DSSCs) have been fabricated from TiO<sub>2</sub>/ZnO nanocomposite which was synthesized by a new green method and pigments (methylene blue as a chemical dye and chlorophyll as a natural dye). These DSSCs were characterized by their high ability to absorb ultraviolet energy, where the efficiency of energy conversion  $\eta$  of ITO-TiO<sub>2</sub>/ZnO were approximately 2.08, and 3.04% with chlorophyll and methylene blue, respectively, showing that  $\eta$  of ITO-TiO<sub>2</sub>/ZnO with methylene blue was the best.

**Keywords:** DSSCs; electrochemical; nanocomposites; titanium dioxide; zinc oxide

### ■ INTRODUCTION

Nanoparticles are the most intriguing materials in nanoscience and technology, which have been applied in photocatalysis, gas sensing, and photovoltaics processes. [1]. Titanium oxide (TiO<sub>2</sub>) and zinc oxide (ZnO) were chosen in this study to fabricate nanocomposites due to their good conductive properties, where TiO<sub>2</sub> anatase and ZnO both exhibit significant exciton binding energies of 60 MeV and band gaps of 3.4 and 3.2 eV, respectively, at ambient temperature [2]. Additionally, because the reasonably priced, non-toxic, and environmentally friendly, they also have good thermal and chemical stability. Also, because of the high band gap, both TiO<sub>2</sub> and ZnO have dye-sensitized solar cells with tapered light response ranges that are only confined to UV [3]. Rapid electron-hole pair recombination is the major issue with isolated TiO<sub>2</sub> and ZnO, which has a negative influence on the substance's photocatalytic activity. TiO<sub>2</sub> and transition metal oxide can be joined to produce composites with significantly higher photocatalytic activity, such as ZnO/TiO<sub>2</sub> [4-5] and Cu<sub>2</sub>O/TiO<sub>2</sub> [6]. This is what was studied in this research.

TiO<sub>2</sub> and ZnO nanoparticles can be synthesized using a variety of techniques, including co-precipitation, sol-gel deposition, electrochemistry, solution combustion, and solid-state reaction. An electrochemical deposition method was used in this study, which produced nanocomposites quickly, easily, cheaply, and with high purity compared to other techniques [7]. Dye-sensitized solar cells (DSSCs) are among the thin-film solar cells that have been an important focus of research for more than two decades due to their simple preparation technique and ease of fabrication as well as their low cost and minimal toxicity [8].

It is a method by which a semiconductor's additional sensitization having a considerable bandgap to the visible region is done by incorporating pigments at the molecular level. By pigment photosensitization, the light absorption spectrum of catalysts can be expanded, and it furthermore amplifies the photon harvesting efficiency by providing additional excited electron pairs from the pigment molecule, which accelerate the transfer of charge. Significant requirements for suitable pigments include an extended

absorption spectrum range and strong adsorption onto the surface of the semiconductor, excited states with longevity and heightened quantum product, and comparable band structure to decrease energy loss in the electron transfer process. The mechanism of dye sensitization even depends on the type of light (rays) [9].

In this study, chlorophyll as a natural dye and methylene blue (MB) as a chemical dye were utilized to generate electricity by applying photovoltaic solar cells. The reason for choosing MB is that it is cheap, available, easy to prepare, and does not cause harm to humans. It has been used as a sunscreen for human skin to reduce UV damage [10]. The maximum absorption wavelength of MB at 665 nm. As well as its strong absorption power, photon absorption allows visible light to be carried by the dye as the electron transfers to the TiO<sub>2</sub>/ZnO nanocomposites [11]. On the other hand, chlorophyll is a green dye found in green plant leaves due to their capacity to absorb red and blue light. It has the greatest absorption at wavelength 670 nm. Furthermore, it contains three carboxylate groups in a molecule without heavy metal ions and is regarded as an environmentally friendly photosensitizer [12].

## ■ EXPERIMENTAL SECTION

### Materials

All materials and solvents utilized in this research were used as such without further purifications where titanium foil (99%) and zinc foil (97%) were obtained from Baoji Jinsheng Metal Material Company. Potassium chloride (96%), and polyvinyl alcohol (PVA) were supplied from Fluka company. Graphite electrode was obtained from Graphite indea limited company. Acetone (98%), ethanol (99%), polyethylene glycol (PEG, 97%), and potassium iodide (97%) were provided from CDH. Iodine (99%) was obtained from Thomas Baker. Deionized water (DW) was obtained from OneMed, methylene blue dye (98%) was obtained from Alfa Aesar, natural eucalyptus leaves and ITO glass (76.2 × 25.4 × 1.1 mm, 11–15 Ω) were obtained from redox. Me company.

### Instrumentation

TiO<sub>2</sub>/ZnO was characterized using XRD (PANalytical AERI), UV-vis spectrophotometer

(Shimadzu UV-1650), FESEM (INSPECT F50), EDX (Thermo Axia), AFM (Naio, Nanosurf AG), and TEM (EM 208S).

### Procedure

#### Preparation of TiO<sub>2</sub>/ZNO nanocomposites

The TiO<sub>2</sub>/ZnO nanocomposite was synthesized by the electrochemical method using the active electrode (anode), which is an electrode made of titanium and zinc foil, and the inert electrode (cathode), which is a graphite electrode as shown in Fig. 1. A power source was also used. The anode and cathode were cleaned with ethanol and acetone before being rinsed with DW [13]. The electrochemical cell was filled with a 200 mL electrolyte solution consisting of 5 mL of 10% (w/v) KCl and 10 mL of 10% (w/v) PVA (stabilizer agent), and the remaining volume of the electrolyte solution was complete with deionized water. In addition, the active electrode consisted of connected pieces of zinc foil (0.75 cm × 4 cm) and titanium foil (1 cm × 4 cm), which were placed face-to-face with a graphite electrode (2 cm × 5 cm) and subsequently immersed in the cell electrolyte [14]. The electrolysis process was carried out in an undivided electrolytic cell and stirred at 30 °C for about 60 min at 20 V. The TiO<sub>2</sub>/ZnO precipitate resulting from this process was centrifuged then rinsed several times with ethanol absolute and DW, and then placed in a drying oven where it was dried for about 60 min at 70 °C before it was calcined at 700 °C for around 60 min [15].



**Fig 1.** The electrochemical apparatus used to prepare the TiO<sub>2</sub>/ZnO nanocomposites

### Fabrication of DSSCs

ITO glass was carefully cleaned with ethanol and DW before being dried with air to remove impurities. The following method was used to design a chemically and naturally dye-sensitive solar cell. A few drops of PEG were added to a small amount of TiO<sub>2</sub>/ZnO nanocomposite to make a colloidal solution (photoanode). While the counter electrode was made of graphite powder and a few drops of PEG, the photoanode and the counter electrode were annealed at 300 °C for around 2 h. The photoanode was placed in a chemical dye solution of 0.5% (w/v) MB by the same method, but another photoanode was put in a chlorophyll dye solution extracted from eucalyptus leaves [16]. Then, both electrodes are placed in the dark for about 7–12 h. Then, it is cleaned using ethanol and DW. Finally, 2–3 drops of an electrolyte solution of 0.1 M iodine (10 g of KI and 3.715 g of I<sub>2</sub> in 250 mL DW) are placed between the two electrodes and the solar cell efficiency is determined [17]. Fig. 2 and 3 show the schematic diagram and design of DSSCs in this work.

## RESULTS AND DISCUSSION

### XRD Analysis for TiO<sub>2</sub>/ZnO Nanocomposites

The XRD patterns of the TiO<sub>2</sub>/ZnO nanocomposite revealed an overlap between the peaks located in the same or neighboring region for both TiO<sub>2</sub> and ZnO NPs, while some peaks appear isolated where there is no overlap between them. These peaks are different in intensity, as shown in Fig. 4. The diffraction peaks have been showing at 2θ of 29.96°, 42.82°, 49.08°, 52.96°, and 61.97° related to the Miller indices (110), (111), (200), (105), and (204), respectively, of TiO<sub>2</sub> anatase and rutile phases (JCPDS No. 89-4921) [18], while other peaks were appearances at 2θ of 31.86°, 34.51°, 36.37°, 47.62°, 56.73°, 66.48°, 68.13°, 69.15°, 72.51°, and 77.05° which associate to the Miller indices (100), (002), (101), (102), (110), (200), (112), (201), (004) and (202), respectively, from the hexagonal wurtzite of ZnO phases (JCPDS No. 36-1451) [19]. A single diffraction peak (2θ) was 35. Meanwhile, peak at 23° indicated the hexagonal crystalline phases of ZnTiO<sub>3</sub> (JCPDS No. 85-05470) [20] because Zn<sup>2+</sup> ions were replaced by Ti<sup>4+</sup> ions. The highest reflection peak is observed at 2θ (36.37°), indicating the small incorporation of the Ti atom

into the ZnO lattice and the ZnO peaks were more intense and shifted towards the higher angle due to the ionic radius mismatch between Zn (0.75 Å) and Ti (0.61 Å) [21]. Consequently, the TiO<sub>2</sub>/ZnO nanocomposites are produced by decreasing the intensity of diffraction angles in some peaks and increasing them in other peaks. Through the XRD technique, the average crystal size of TiO<sub>2</sub>/ZnO nanocomposites can be calculated using Scherrer's (Eq. (1)), where it was 37 nm because the variables of this equation obtained XRD data;

$$D = \frac{k\lambda}{FWHM \cos\theta} \quad (1)$$

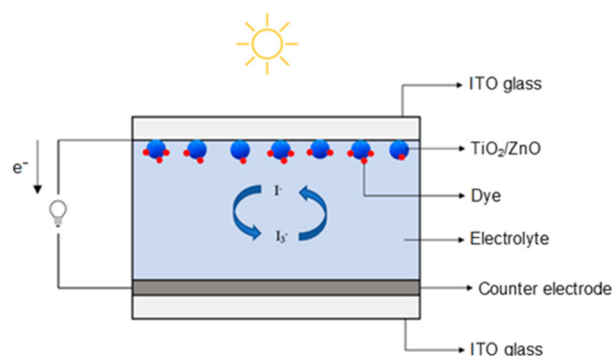


Fig 2. Schematic diagram of a DSSC

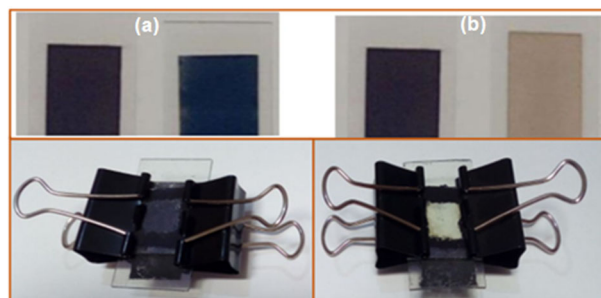


Fig 3. Design of (a) chemical and (b) natural dye DSSCs

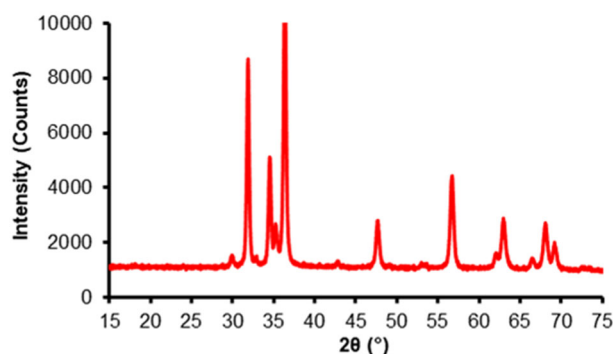


Fig 4. XRD pattern of TiO<sub>2</sub>/ZnO nanocomposites

where  $D$  is the size of the crystals,  $\theta$  is the Bragg diffraction angle, FWHM is the full width of the diffraction peak at half maximum,  $\lambda$  is the wavelength of Cu-K $\alpha$  radiation (0.15406 nm), and  $K$  is a constant (0.9) [22].

### TEM Analysis for TiO<sub>2</sub>/ZnO Nanocomposites

TEM micrographs of the TiO<sub>2</sub>/ZnO nanocomposites provide evidence of the ZnO nanoparticle's rod-like morphology. Moreover, the TiO<sub>2</sub> NPs have a spherical morphology and very small diameters. Additionally, it was found that some of the TiO<sub>2</sub> NPs adhered to the ZnO surface, while others were embedded in the ZnO NPs, which is illustrated in Fig. 5, and these findings are consistent with previous study results [23]. Statistical results showed that the mean particle size of TiO<sub>2</sub>/ZnO nanocomposites at 100 and 50 nm scales were 43.14 and 21.16 nm, respectively. This is additional evidence for the preparation of TiO<sub>2</sub>/ZnO nanocomposites.

### FESEM for TiO<sub>2</sub>/ZnO Nanocomposites

The morphological and structural characteristics of TiO<sub>2</sub>/ZnO nanocomposites were observed using FESEM.

Fig. 6 indicated that the NPs were prepared in the nanometer range and some of the NPs were well separated from each other, while most of them were present in the agglomerated form of tiny crystals. This agglomeration is due to electrostatic effects, which reveals that this agglomeration behavior of NPs is consistent with a behavior similar to the agglomeration of NPs in previous studies [24-25]. In addition, they provide evidence of ZnO NPs' rod-like morphology. While the TiO<sub>2</sub> NPs have a spherical morphology and very small diameters. Statistical results showed that the mean particle size of TiO<sub>2</sub>/ZnO nanocomposites at 500 nm and 3  $\mu$ m were 98.14 nm and 0.250  $\mu$ m, respectively.

### EDX for TiO<sub>2</sub>/ZnO Nanocomposites

The purity and stoichiometry of the electrochemically produced TiO<sub>2</sub>/ZnO nanocomposites were evaluated using EDX. Fig. 7 reveals the presence of unique signals for O, Ti, and Zn elements, providing proof that the samples were highly pure. The mol ratio of TiO<sub>2</sub>/ZnO is (Zn = 14.2%, Ti = 16.3%, O = 49.8%), and

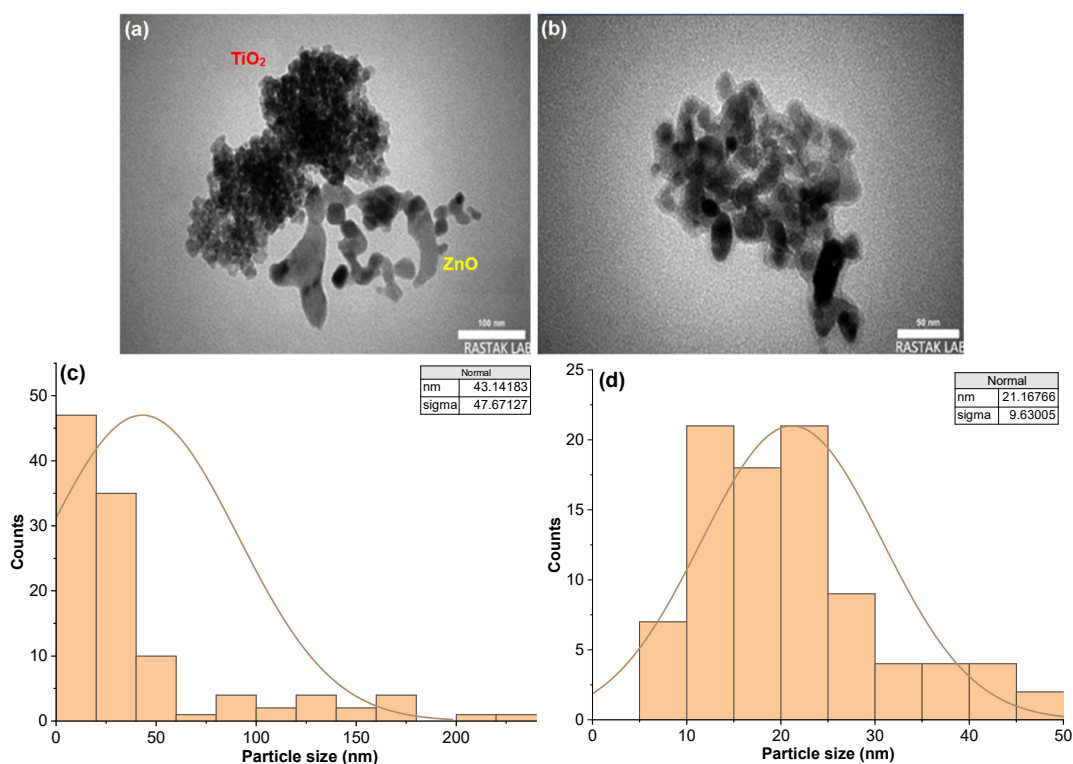


**Fig 5.** TEM images and size distribution graphs of TiO<sub>2</sub>/ZnO nanocomposites at different scales (a, c) at 100 nm and (b, d) at 50 nm

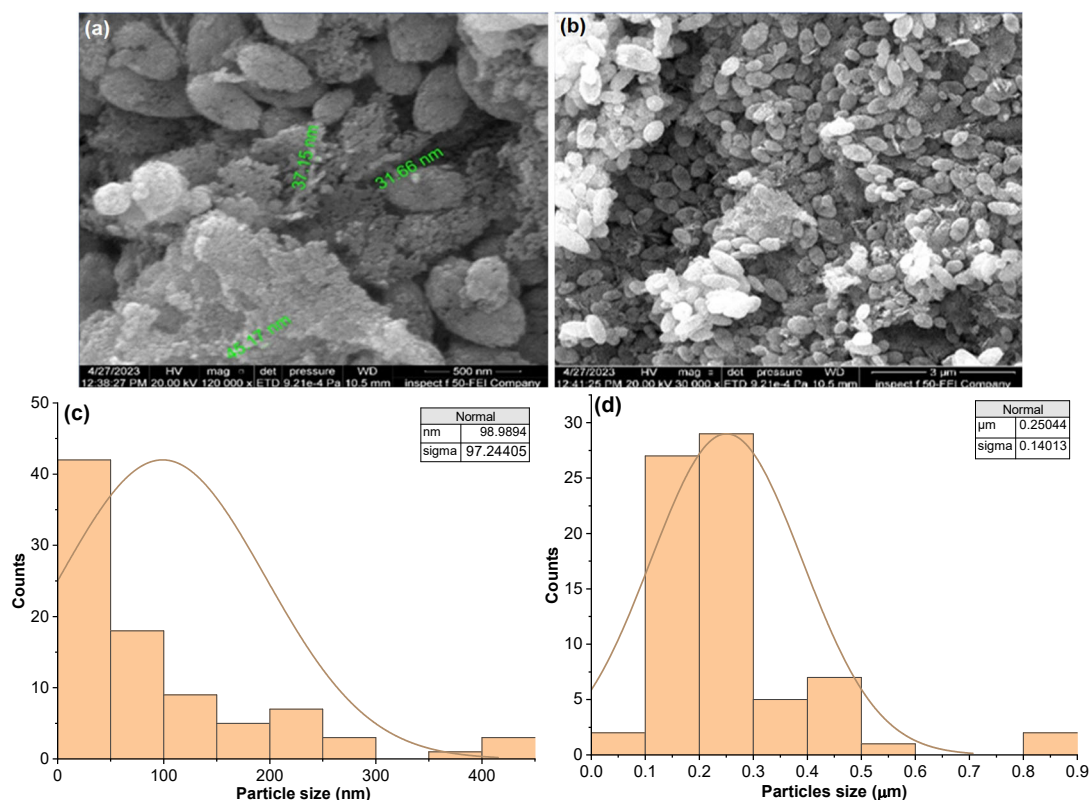


**Fig 6.** FESEM images and size distribution graphs of TiO<sub>2</sub>/ZnO nanocomposites at different scales (a, c) at 500 nm and (b, d) at 3 μm

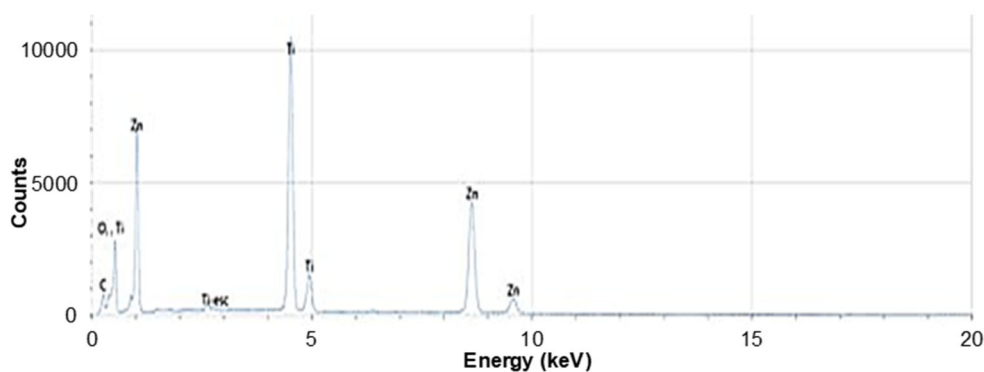


**Fig 7.** EDX spectrum of TiO<sub>2</sub>/ZnO nanocomposites

the weight percentages of TiO<sub>2</sub>/ZnO are (Zn = 32.2%, Ti = 27.9%, O = 30.7%). These ratios demonstrate that the ratio of TiO<sub>2</sub>:ZnO was 1:1.

#### AFM Analysis for TiO<sub>2</sub>/ZnO Nanocomposites

The nanocomposites of TiO<sub>2</sub>/ZnO were diagnosed using AFM. The morphology observed that the surface 3D consists of an aggregation of granules called clusters. This indicates good homogeneity as shown in Fig. 8. The measurements included a mean diameter of 37.2 nm,

which is compatible with the results obtained from the XRD pattern, mean height of 8 nm, and roughness analyses such as root mean square ( $S_q$ ) of 6.84 nm, limit the maximum height ( $S_z$ ) of 82.75 nm, arithmetic mean height ( $S_a$ ) is 5.24 nm, and surface area ratio ( $S_{ar}$ ) of 1.524. On the other hand, AFM measurements supply excellent information on the size distribution, homogeneity of NP surfaces, and the mean diameter of nanoparticles [26].

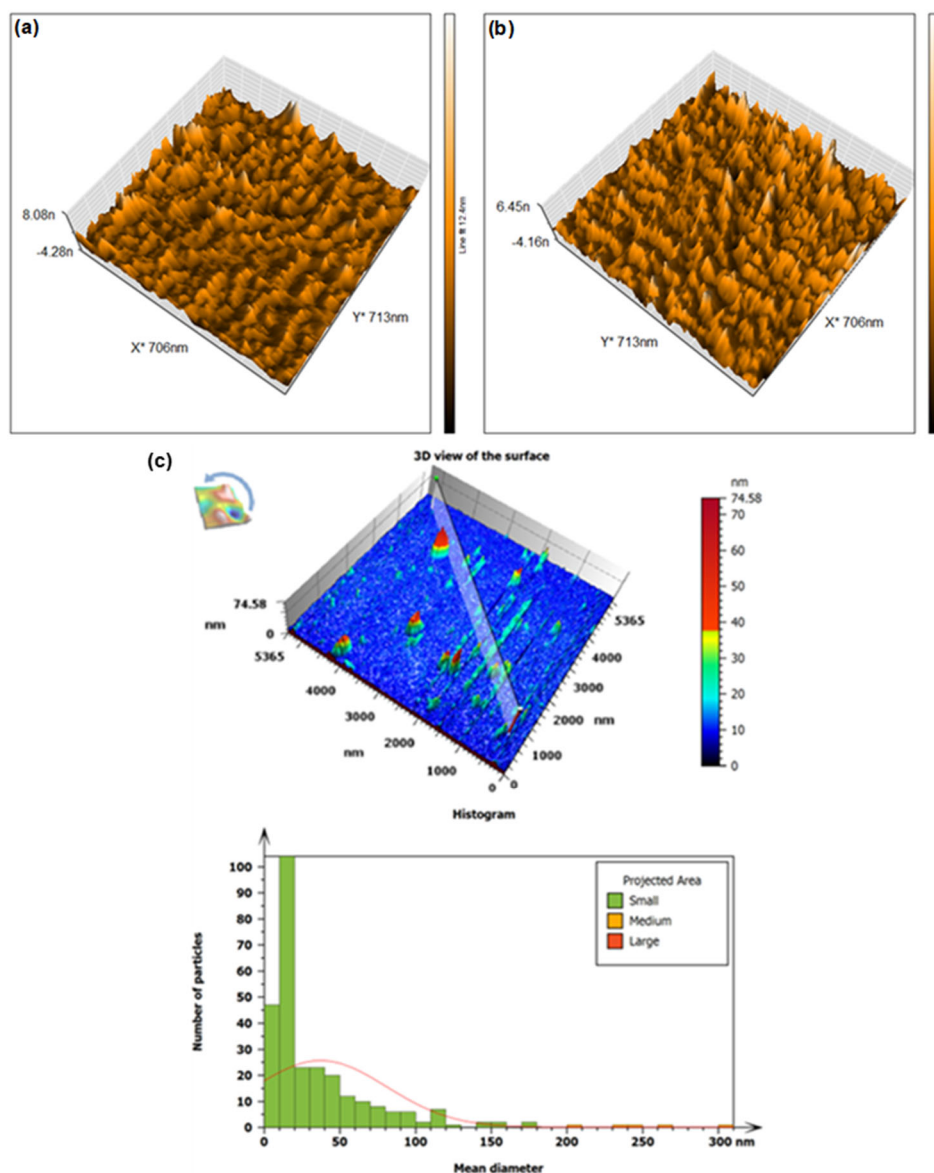


Fig 8. AFM (a, b) 3D image scales, and (c) particle analysis of TiO<sub>2</sub>/ZnO nanocomposites

### UV-vis Study of TiO<sub>2</sub>/ZnO Nanocomposite

Nanocomposite thin films of TiO<sub>2</sub>/ZnO were made of glass slides at room temperature and analyzed with solid-state UV-vis spectroscopy. Fig. 9 shows  $\lambda_{\max}$  obtained was around 395 nm, and the energy band gap was calculated by the Tauc. relation (Eq. (2)) [27];

$$\alpha h\nu^{1/n} = k(h\nu - E_g) \quad (2)$$

where k is a constant,  $\alpha$  is the molar extinction coefficient,  $h\nu$  is the incident photon energy in (eV),  $E_g$  is the optical energy band gap, and n is index depending on the type of transition. The band gap was estimated from the

intersection of the two lines part of  $(\alpha h\nu)^2$  plots vs.  $h\nu$ . The equation is a direct band gap. Based on this equation, the bandgap value of TiO<sub>2</sub>/ZnO is 3.13 eV as shown in Fig. 10, which indicates that TiO<sub>2</sub>/ZnO is a semiconductor because the calculated energy gap value (3.13 eV) is less than 4.0 eV [28].

### The DSSCs Parameter

The following formula (Eq. (3)) was used to calculate the solar cell's energy conversion efficiency ( $\eta$ );

$$\eta = \frac{P_{\max}}{P_{\text{in}}} = \frac{V_{\text{oc}} J_{\text{sc}} \text{FF}}{P_{\text{in}}} \times 100\% \quad (3)$$

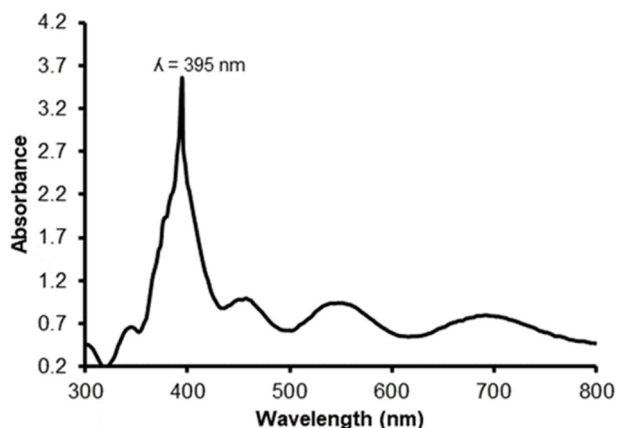


Fig 9. UV-vis spectrum of TiO<sub>2</sub>/ZnO nanocomposites

where  $P_{\max}$  is the maximum power output,  $V_{oc}$  is a photovoltaic open circuit,  $J_{sc}$  is short circuit density, and  $P_{in}$  is a lamp power incident which is equal to (40 mW/cm<sup>2</sup>). Additionally, the fill factor (FF) is represented by Eq. (4);

$$FF = \frac{V_{\max} J_{\max}}{V_{oc} J_{sc}} \quad (4)$$

where  $J_{\max}$  is the current density, and  $V_{\max}$  is the maximum output voltage. The characteristics of the solar cell are  $V_{oc} = 0.53$  &  $0.56$  V,  $J_{sc} = 4.2$  &  $6.7$  mA/cm<sup>2</sup>,  $V_{\max} = 0.32$  &  $0.32$  V,  $J_{\max} = 2.6$  &  $3.8$  mA/cm<sup>2</sup>,  $FF = 0.373$  &  $0.324$ , and the conversion efficiency is 2.08 & 3.04% for TiO<sub>2</sub>/ZnO with chlorophyll and MB dyes, respectively. The enhanced solar efficiency of using natural dye is attributed to auxochrome groups of chlorophyll dye, such as carbonyl (C=O) groups, which supply the ability to absorb light in a visible spectrum from the sunlight. Thus, these

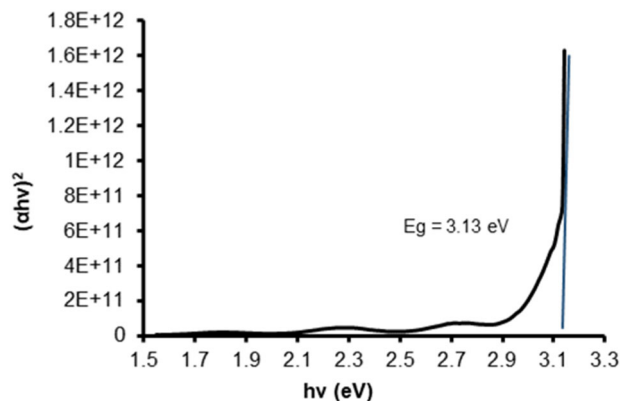


Fig 10. Tauc plot graph of the optical band gap energy of TiO<sub>2</sub>/ZnO nanocomposites

auxochrome groups can be connected to the Zn(II) and Ti(IV) position of the TiO<sub>2</sub>/ZnO surface in favor of the electron transfer from the chlorophyll molecules to the TiO<sub>2</sub>/ZnO conduction band. In addition, chlorophylls possess a porphyrin ring, which serves as a suitable light-harvesting antenna for assembling solar energy. Consequently, TiO<sub>2</sub>/ZnO with porphyrin has been a good sensitizer for achieving photocatalysis of visible light [29]. While enhancing solar efficiency by use of chemical dye (MB) is due to the occurrence of an electron transfer from the dye of TiO<sub>2</sub>/ZnO to composite, and the results showed higher efficiency of the MB dye compared to the pigment chlorophyll, this was attributed to the synergetic effect of the phase junction of MB and TiO<sub>2</sub>/ZnO nanocomposite, which reduces the recombination of photoexcited electron-hole pairs [30]. Additionally, due to the difficulty of fixing the natural dye

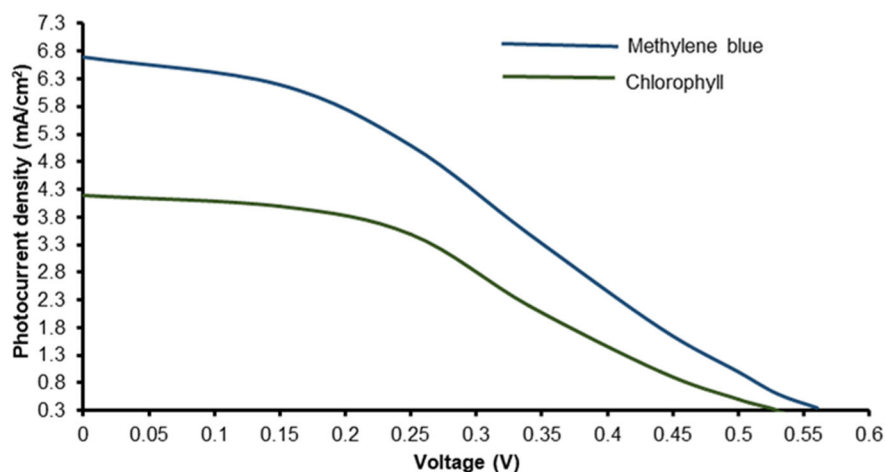


Fig 11. J-V curve for the DSSC

on the semiconductor surface, as well as the presence of alkyl and vinyl groups in the structure, this causes a steric barrier that prevents chlorophyll molecules from interacting with TiO<sub>2</sub>/ZnO [31], Fig. 11 shows the working electrode for the dye-sensitized solar cell, which is based on a synthetic TiO<sub>2</sub>/ZnO nanocomposite.

## ■ CONCLUSION

DSSCs with high efficiency in producing electrical energy were prepared from TiO<sub>2</sub>/ZnO nanocomposite safely and highly efficiently prepared from available and cheap raw materials and by a safe, easy and fast (electrochemical method). The FESEM, TEM, and AFM images indicated that samples revealed a well-ordered and good-sized distribution of particles. Meanwhile, the results of XRD and AFM techniques showed a nanoparticle synthesized in a small size. Also, the energy band gap was measured by the use of UV-vis techniques. Dyes with high sensitivity to light were used to improve the efficiency of the cell, where the efficiency of energy conversion  $\eta$  of ITO-TiO<sub>2</sub>/ZnO was approximately 2.08 and 3.04% with chlorophyll and MB, respectively. It will search in the future for the possibility of fabricating more efficient cells from natural materials.

## ■ ACKNOWLEDGMENTS

The authors would like to thank all the staff in the consulting engineering office laboratories in the College of Engineering, University of Kufa.

## ■ AUTHOR CONTRIBUTIONS

The first researcher contributed to proposing the project idea, interpreting the analytical data, and reviewing the research, and the second researcher contributed to implementing the research project, writing the manuscript, and interpreting the results.

## ■ REFERENCES

- [1] Suharyadi, S., Syauqi, M.I., Amelia, P., Yunita, Y., and Gunlazuardi, J., 2023, Dye-sensitized solar cell photoelectrochemical tandem system performance study: TiO<sub>2</sub> nanotube/N719, BiVO<sub>4</sub>/TiO<sub>2</sub> nanotube, Ti<sup>3+</sup>/TiO<sub>2</sub> nanotube for nitrogen reduction reaction to ammonia, *Indones. J. Chem.*, 23 (3), 583–593.
- [2] Munguti, L., and Dejene, F., 2021, Effects of Zn:Ti molar ratios on the morphological, optical and photocatalytic properties of ZnO-TiO<sub>2</sub> nanocomposites for application in dye removal, *Mater. Sci. Semicond. Process.*, 128, 105786.
- [3] Kumar, U., Hassan, J.Z., Bhatti, R.A., Raza, A., Nazir, G., Nabgan, W., and Ikram, M., 2022, Photocatalysis vs adsorption by metal oxide nanoparticles, *J. Mater. Sci. Technol.*, 131, 122–166.
- [4] Ji, L., Li, J., Lei, J., Ren, Y., Zhou, S., and Liang, L., 2023, Preparation and characterization of Cu<sup>2+</sup>/ZnO/TiO<sub>2</sub> nanocomposites for the treatment of typical benzene series in oilfield produced water, *Catal. Commun.*, 174, 106572.
- [5] Thate, A.G., Pakhare, K.S., Patil, S.S., and Bhuse, V.M., 2023, Fabrication of TiO<sub>2</sub>-ZnO nanocomposite photoanodes to enhance the dye-sensitized solar cell efficiency, *Res. Chem. Intermed.*, 49 (1), 147–168.
- [6] Zhang J., Zhou, Z., Xiao, B., Zhou, C., Jiang, Z., Liang, Y., Sun, Z., Xiong, J., Chen, G., Zhu, H., and Wang, S., 2023, Visible-light photocatalytic degradation of water-soluble polyvinyl alcohol in aqueous solution by Cu<sub>2</sub>O@TiO<sub>2</sub>: Optimization of conditions, mechanisms and toxicity analysis, *J. Environ. Manage.*, 341, 118054.
- [7] Estévez Ruiz, E.P., Lago, J.L., and Thirumuruganandham, S.P., 2023, Experimental studies on TiO<sub>2</sub> NT with metal dopants through coprecipitation, sol-gel, hydrothermal scheme and corresponding computational molecular evaluations, *Materials*, 16 (8), 3076.
- [8] Prajapat, K., Dhonde, M., Sahu, K., Bhojane, P., Murty, V.V.S., and Shirage, P.M., 2023, The evolution of organic materials for efficient dye-sensitized solar cells, *J. Photochem. Photobiol., C*, 55, 100586.
- [9] Setiarso, P., Harsono, R.V., and Kusumawati, N., 2023, Fabrication of dye sensitized solar cell (DSSC) using combination of dyes extracted from curcuma (*Curcuma xanthorrhiza*) rhizome and binahong (*Anredera cordifolia*) leaf with treatment in pH of the extraction, *Indones. J. Chem.*, 23 (4), 924–936.

- [10] Xiong, Z.M., Mao, X., Trappio, M., Arya, C., el Kordi, J., and Cao, K., 2021, Ultraviolet radiation protection potentials of methylene blue for human skin and coral reef health, *Sci. Rep.*, 11 (1), 10871.
- [11] Nurhidayani, N., Muzakkar, M.Z., Maulidiyah, M., Wibowo, D., and Nurdin, M., 2017, A novel of Buton asphalt and methylene blue as dye-sensitized solar cell using TiO<sub>2</sub>/Ti nanotubes electrode, *IOP Conf. Ser.: Mater. Sci. Eng.*, 267 (1), 012035.
- [12] Omar, A., Ali, M.S., and Abd Rahim, N., 2020, Electron transport properties analysis of titanium dioxide dye-sensitized solar cells (TiO<sub>2</sub>-DSSCs) based natural dyes using electrochemical impedance spectroscopy concept, *Sol. Energy*, 207, 1088–1121.
- [13] Micó-Vicent, B., Perales Romero, E., Jordán-Núñez, J., and Viqueira, V., 2021, Halloysite and laponite hybrid pigments synthesis with copper chlorophyll, *Appl. Sci.*, 11 (12), 5568.
- [14] How, Y.Y., Numan, A., Mustafa, M.N., Walvekar, R., Khalid, M., and Mubarak, N.M., 2022, A review on the binder-free electrode fabrication for electrochemical energy storage devices, *J. Energy Storage*, 51, 104324.
- [15] El-Khawaga, A.M., Zidan, A., and Abd El-Mageed, A.I.A.A., 2023, Preparation methods of different nanomaterials for various potential applications: A review, *J. Mol. Struct.*, 1281, 135148.
- [16] Anand, A., Mittal, S., Leeladevi, V., and De, D., 2023, Nanoflower shaped ZnO photoanode and natural dye sensitizer based solar cell fabrication, *Mater. Today: Proc.*, 72, 227–231.
- [17] Mahdi Rheima, A., Hadi Hussain, D., and Jawad Abed, H., 2020, Fabrication of a new photo-sensitized solar cell using TiO<sub>2</sub>/ZnO nanocomposite synthesized via a modified sol-gel Technique, *IOP Conf. Ser.: Mater. Sci. Eng.*, 928 (5), 052036.
- [18] He, J., Liu, Q., Zhang, Y., Zhao, X., Zhang, G., Xiao, B., and Fu, K., 2023, *In situ* synthesis of the mesoporous C-TiO<sub>2</sub> microspheres derived from partial hydrolysis tetrabutyl titanate for enhanced photocatalytic degradation under visible light, *Mater. Res. Bull.*, 161, 112168.
- [19] Fu, Y., Ba, S., Feng, L., Xia, P., Sun, W., Zhang, B., Zhao, Y., Tian, J., and Wang, F., 2023, Study on the catalytic performance of a new double-shell composite energetic material, *J. Phys.: Conf. Ser.*, 2566 (1), 012001.
- [20] Ali, M.M., Haque, M.J., Kabir, M.H., Kaiyum, M.A., and Rahman, M.S., 2021, Nano synthesis of ZnO-TiO<sub>2</sub> composites by sol-gel method and evaluation of their antibacterial, optical and photocatalytic activities, *Results Mater.*, 11, 100199.
- [21] Baitha, P.K., and Manam, J., 2016, Luminescence properties of ZnO/TiO<sub>2</sub> nanocomposite activated by Eu<sup>3+</sup> and their spectroscopic analysis, *Bull. Mater. Sci.*, 39 (5), 1233–1243.
- [22] Zeinali Heris, S., Etemadi, M., Mousavi, S.B., Mohammadpourfard, M., and Ramavandi, B., 2023, Preparation and characterizations of TiO<sub>2</sub>/ZnO nanohybrid and its application in photocatalytic degradation of tetracycline in wastewater, *J. Photochem. Photobiol., A*, 443, 114893.
- [23] Hellen, N., Park, H., and Kim, K.N., 2018, Characterization of ZnO/TiO<sub>2</sub> nanocomposites prepared via the sol-gel method, *J. Korean Ceram. Soc.*, 55 (2), 140–144.
- [24] Harrum, W.M.W., Akhir, R.M., Afaah, A.N., Eswar, K.A., Husairi, F.S., Rusop, M., and Khusaimi, Z., 2023, Comparative study of surface, elemental, structural and optical morphologies of titanium dioxide-zinc oxide (TiO<sub>2</sub>-ZnO) and titanium dioxide-zinc oxide/graphene (TiO<sub>2</sub>-ZnO/Gn), *Mater. Today: Proc.*, 75, 147–150.
- [25] Hongxia, J., Yanlin, G., Longxiang, L., Xu, W., and Wangjun, P., 2023, A new double Z-scheme TiO<sub>2</sub>/ZnO-g-C<sub>3</sub>N<sub>4</sub> nanocomposite with enhanced photodegradation efficiency for Rhodamine B under sunlight, *Environ. Prog. Sustainable Energy*, 42 (1), e13968.
- [26] Kumar, A., Nayak, D., Sahoo, P., Nandi, B.K., Saxena, V.K., and Thangavel, R., 2023, Fabrication of porous and visible light active ZnO nanorods and ZnO@TiO<sub>2</sub> core-shell photocatalysts for self-cleaning applications, *Phys. Chem. Chem. Phys.*, 25 (24), 16423–16437.
- [27] Tauc, J., 1968, Optical properties and electronic structure of amorphous Ge and Si, *Mater. Res. Bull.*, 13 (1), 37–46.

- [28] Mancuso, A., Blangetti, N., Sacco, O., Freyria, F.S., Bonelli, B., Esposito, S., Sannino, D., and Vaiano, V., 2023, Photocatalytic degradation of crystal violet dye under visible light by Fe-doped TiO<sub>2</sub> prepared by reverse-micelle sol-gel method, *Nanomaterials*, 13 (2), 270.
- [29] Krishnan, S., and Shriwastav, A., 2021, Application of TiO<sub>2</sub> nanoparticles sensitized with natural chlorophyll pigments as catalyst for visible light photocatalytic degradation of methylene blue, *J. Environ. Chem. Eng.*, 9 (1), 104699.
- [30] Buu, T.T., Son, V.H., Nam, N.T.H., Hai, N.D., Vuong, H.T., Quang, L.T.K., Dat, N.M., Lin, T.H., Phong, M.T., and Hieu, N.H., 2023, Three-dimensional ZnO-TiO<sub>2</sub>/graphene aerogel for water remediation: The screening studies of adsorption and photodegradation, *Ceram. Int.*, 49 (6), 9868-9882.
- [31] Munandar, M.R., Hakim, A.S.R., Puspitadinda, H.A., Andiyani, S.P., and Nurosyid, F., 2022, The effect of mixing chlorophyll-antocyanin as a natural source dye on the efficiency of dye-sensitized solar cell (DSSC), *J. Phys.: Conf. Ser.*, 2190 (1), 012042.